Available online at www.sciencedirect.com

ScienceDirect

Mendeleev Commun., 2022, **32**, 591–593

Mendeleev Communications

Synthesis and evaluation of the anticancer activity of the water-dispersible complexes of 4-acylaminoisoxazole derivative with biocompatible nanocontainers based on Ca^{2+} (Mg^{2+}) cross-linked alginate

Vasily V. Spiridonov,*[a] Kirill S. Sadovnikov,[a] Dmitry A. Vasilenko,[a] Kseniya N. Sedenkova,[a] Alina R. Lukmanova,[b] Alina A. Markova,[c,d] Anna V. Shibaeva,[c] Anastasia V. Bolshakova,[a] Sergey S. Karlov,[a] Elena B. Averina*[a] and Alexander A. Yaroslavov[a]

[a] *Department of Chemistry, M. V. Lomonosov Moscow State University, 119991 Moscow, Russian Federation. E-mail: vasya_spiridonov@mail.ru, elaver@med.chem.msu.ru*

[b] *Department of Materials Science, M. V. Lomonosov Moscow State University, 119991 Moscow, Russian Federation*

[c] *N. M. Emanuel Institute of Biochemical Physics, Russian Academy of Sciences, 119991 Moscow, Russian Federation*

[d] *A. N. Nesmeyanov Institute of Organoelement Compounds, Russian Academy of Sciences, 119991 Moscow, Russian Federation*

DOI: 10.1016/j.mencom.2022.09.007

Water-dispersible complexes of 4-methyl-*N*-[5-methyl-3-(3,4,5-trimethoxyphenyl)isoxazol-4-yl]benzamide possessing anticancer activity were prepared by its immobilization with biocompatible polymer nanocontainers based on sodium alginate cross-linked with Ca^{2+} and Mg^{2+} ions. It was found that this isoxazole derivative retains its structure during immobilization. Colloidal stable nanocontainers filled with this compound exhibit toxicity toward the colon carcinoma (HCT116) tumor cell line.

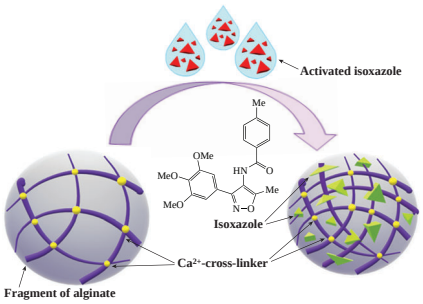

Keywords: polysaccharide nanocontainers, alginate, 4-acylaminoisoxazoles, colloidal stability, anticancer activity.

Isoxazole derivatives represent an important class of N,O-heterocyclic compounds which has found numerous applications in organic and medicinal chemistry.[1–6] Isoxazole moiety is of particular interest as a core of natural products (*e.g.*, ibotenic acid, muscimol), marketed drugs (oxacillin, valdecoxib, isocarboxazid and many others) and compounds with a broad range of biological activities.[7–12] Also, isoxazole derivatives have found application in design of drug candidates for cancer therapy.[13–18] Isoxazole derivatives containing various substituents and functional groups are generally characterized by high hydrophobicity. So, they are poorly soluble in aqueous media, that limits the possibilities for their biomedical application. Due to this fact, as well as to the ability of isoxazoles to exert a toxic effect not only on cancer, but also on normal cells, the problem of obtaining water-dispersible forms of isoxazole derivatives and their controlled administration only to cancer cells is extremely relevant.

In our previous publication, we have shown that 4-methyl-*N*-[5-methyl-3-(3,4,5-trimethoxyphenyl)isoxazol-4-yl]benzamide **1** demonstrated high anticancer activity on a series of cancer cell lines but revealed low selectivity in comparison to normal cells.[18] Also, the significant disadvantage of this compound is poor solubility in water. To eliminate these shortcomings, in the present work we propose an approach consisting in the immobilization of isoxazole **1** with a polymer carrier. As polymer carriers, natural water-dispersible biocompatible nanocontainers based on the sodium salt of alginic acid, cross-linked with Ca^{2+} and Mg^{2+} ions, were used.

In order to immobilize isoxazole **1** with nanocontainers, it was proposed to preliminarily transform it from a neutral molecule into a charged (protonated) form **1′** (Scheme 1), which may electrostatically interact with carboxy groups of anionic nanocontainers.

The formation of polysaccharide nanocontainers, as well as their interaction with isoxazole **1′**, was controlled by dynamic light scattering (DLS), laser microelectrophoresis, and transmission electron microscopy (TEM). DLS and electrokinetic measurements of specimens were carried out according to the

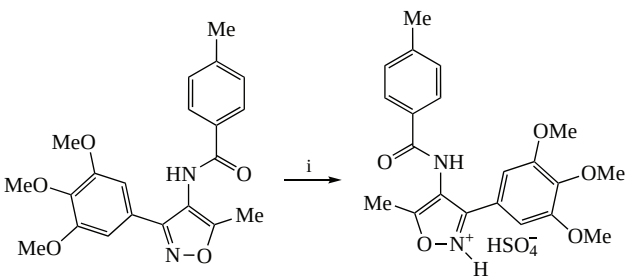

1 **1′**

Scheme 1 *Reagents and conditions*: i, H_2SO_4, 50 °C, 15 min.

procedures described earlier.[19,20] To confirm that the isoxazole ring remains stable under acidic conditions, a control experiment was carried out consisting in the treatment of isoxazole **1** with 50% sulfuric acid, subsequent neutralization of the reaction mixture, isolation of heterocycle **1**, and control with ^{1}H NMR spectroscopy. The quantitative content of protonated isoxazole **1′** in the composition with nanocontainers was determined by UV spectrophotometry. The cytotoxicity of nanocontainers filled with isoxazole **1′** towards both non-tumor and tumor cells was assessed.

A synthesis of nanocontainers cross-linked with Ca^{2+} and Mg^{2+} ions was performed following the described procedure.[19,20] Molar ratio both for [Alginate monomer units]/[Ca^{2+}] and [Alginate monomer units]/[Mg^{2+}] was 10÷1. After purification and lyophilization, white complexes were obtained which were dissolved in water affording Alg–Ca^{2+} **I** and Alg–Mg^{2+} **II** nanocontainers solutions, respectively. To confirm the formation of nanocontainers, the hydrodynamic characteristics of samples **I**, **II** were studied using DLS (Table 1). It was established that the effective hydrodynamic diameter D_h of the initial Alginate macromolecules in an aqueous solution is 680 nm. The interaction of linear Alginate both with Ca^{2+} and Mg^{2+} ions leads to a significant contraction in particle size. For specimens **I** and **II**, the particle diameters are 350 and 370 nm, respectively. The data obtained are in agreement with the results obtained by means of TEM (Figure 1).

TEM image of the nanocontainers **I** contains dark gray particles characterized by spherical symmetry in general. The size (diameter) of individual nanocontainer particles **I** varies from 130 to 190 nm. On the other hand, TEM image of nanocontainers **II** contains similar spherical dark gray particles. The size (diameter) of these individual particles of nanocontainers **II** varies in the range from 120 to 190 nm.

The electrokinetic characteristics of aqueous solutions **I**, **II** were studied by laser microelectrophoresis (see Table 1). All the samples are characterized by negative electrophoretic mobility (EPM) values, which are –3.19 for **I** and –2.41 μm s^{-1} V^{-1} cm for **II**. EPM of initial Na-Alginate is –3.21 μm s^{-1} V^{-1} cm.

It was established that **I**, **II** particles are characterized both by significantly smaller sizes and EPM in comparison with initial linear Alginate macromolecules. This result is explained with a change in the conformation (contraction) of initial Alginate macromolecules due to the formation of electrostatic contacts between fragments of polysaccharide macromolecules through divalent metal ions (Ca^{2+} and Mg^{2+}), accompanied by the formation of a cross-linked structure of particles **I**, **II**.

Isoxazole **1** was immobilized by obtained nanocontainers in two stages. The first step was to prepare the protonated form of isoxazole **1′** using 50% sulfuric acid (the addition of sulfuric acid to isoxazole derivative **1** leads to its complete dissolution). Based on the literature data,[21] we assumed that the protonation of isoxazole **1** with sulfuric acid can occur at the nitrogen atom of the isoxazole ring (see Scheme 1), while additional stabilization of the resulting cation **1′** is possible due to conjugation of the heterocyclic fragment with the 3-positioned aromatic substituent.

The next step was to incorporate species **1′** into the **I**, **II** nanocontainers when acidic solution of **1′** was added to aqueous solution of nanocontainers **I** or **II**. During the interaction of **I**, **II** with **1′**, the weight ratio of isoxazole/nanocontainers = 0.3 was maintained. The resulting mixtures were neutralized up to pH 7 after injection of **1′** acidic solution to the nanocontainers. The resulting solutions were dialyzed and lyophilized; the final products were dissolved in water affording (Alg)–Ca^{2+}-Isoxazole **III** and (Alg)–Mg^{2+}-Isoxazole **IV** particles. The quantity of isoxazole **1′** in **III** and **IV** was determined by UV spectrophotometry (see Online Supplementary Materials). It was established that both **III** and **IV** are able to immobilize 20 wt% isoxazole **1′**. Moreover, the nature of the cross-linking ion does not affect the binding ability of nanocontainers **I** and **II** with respect to **1′**.

Hydrodynamic and electrokinetic characteristics of samples **III** and **IV** were also studied (see Table 1) by DLS and laser microelectrophoresis. Effective diameters of **III** and **IV** were found to be 180 and 190 nm, respectively. Negative EPM values indicate that both **III** and **IV** are characterized by high aggregative stability. To visualize specimens **III** and **IV**, TEM was used. In the field of the microscope the gray spherical particles were found both in case of **III** [Figure 2 **(***a***)**] and **IV** [Figure 2(*b*)]. The average diameters of individual particles were found to be 170 and 160 nm for **III** and **IV**, respectively.

Specimens **III** and **IV** can be of interest for controlled drug delivery to target areas of the body. Such nanocontainers must meet the requirements for carriers of biologically active substances including low toxicity to normal cells. The cytotoxic effect of the compounds was studied by the MTT test towards both non-tumor human fibroblasts and HCT116 (colon

Table 1 Hydrodynamic and electrokinetic characteristics of aqueous dispersions of Ca^{2+} and Mg^{2+} cross-linked nanocontainers.

Parameter	Nanocontainer			
	(Alg)–Ca^{2+} **I**	(Alg)–Mg^{2+} **II**	(Alg)–Ca^{2+}-Izoxazole **III**	(Alg)–Mg^{2+}-Izoxazole **IV**
D_h/nm	350	370	180	185
EPM/ μm s^{-1} V^{-1} cm	–3.19	–2.41	–1.01	–1.31

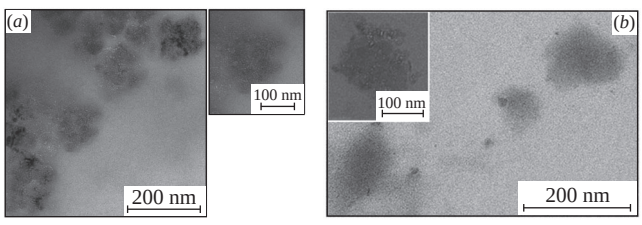

Figure 1 TEM images of (*a*) Ca^{2+} cross-linked nanocontainer, in the upper right corner a detailed image of single particle and of (*b*) Mg^{2+} cross-linked microgel, in the upper left corner a detailed image of single particle.

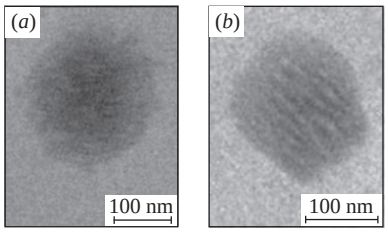

Figure 2 TEM images of (*a*) nanocontainer **III** and (*b*) nanocontainer **IV**.

Table 2 Cytotoxicity of water soluble nanocontainers based on alginate, cross-linked with ions, filled with isoxazole derivative **1′** towards non-tumor and tumor cells.[a]

Specimen	IC_{50}/μM	
	Non-tumor human fibroblasts	HCT116
Isoxazole **1**	0.21	0.18
I	>50	0.1
II	>50	3.25
III	0.31	0.1
IV	3.42	0.22

[a] The measurements were carried out in DMSO-containing solution (final concentration of DMSO < 0.5%).

carcinoma). The percentage of surviving cells corresponding 50% (IC_{50}) was taken as a quantitative measure of cytotoxicity (Table 2).

As shown in Table 2, isoxazole derivative **1** is roughly equally cytotoxic towards both HCT116 colon carcinoma cells and non-tumor fibroblasts. As for the nanocontainers **I** and **II**, they do not demonstrate toxic effect towards non-tumor human fibroblasts, but have noticeable cytotoxicity towards HCT116 cells. It was found that nanocontainers **III** and **IV** filled with isoxazole **1′** possess the close cytotoxicity towards HCT116 cell line, while their cytotoxic effect on non-tumor fibroblasts significantly differs. Thus, the cytotoxicity of nanocontainer **IV** to colon carcinoma cancer cell line HCT116 (IC_{50} = 0.22 μM) was more than one order of magnitude higher than to non-tumor fibroblasts (IC_{50} = 3.42 μM). So, nanocontainer **IV** has significantly better toxicological profile *in vitro* compared to isoxazole derivative **1** and nanocontainer **III**.

The difference between toxicological profiles of nanocontainers **III** and **IV** can be explained as follows. Nanocontainers **III** and **IV** were prepared using Ca^{2+} and Mg^{2+} ions as cross-linking agents, respectively. It is well-known that Ca^{2+} ions are capable of exerting a direct toxic effect on cells.[22] The primary targets of Ca^{2+} ions are mitochondria and the endoplasmic reticulum. Mitochondria can respond to the apoptotic Ca^{2+} signal both by enhance in reactive oxygen species generation and by opening the pores of the inner mitochondrial membrane. Ions Mg^{2+} do not possess described properties. These ions play the role of signals transmitters from outside-inside the cell and exhibit an effector function.[23]

In conclusion, an original approach to prepare a water-dispersible form of isoxazole derivative **1** with antimitotic activity was proposed. The method involves protonation of isoxazole **1** followed by encapsulation in nanocontainers **I** or **II** based on the biocompatible polysaccharide. The maximum content of isoxazole **1′** in nanocontainers is 20 wt%. This value does not depend on the nature of the cross-linking ion. The particle size of **I** and **II** as well as **III** and **IV** varies from 180 to 250 nm. Nanocontainers **I** and **II** demonstrate the absence of toxicity towards non-tumor cells. At the same time, being filled with isoxazole **1′**, nanocontainers **III** and particularly **IV** show less toxicity towards non-tumor fibroblasts through to a protective polysaccharide capsule, but high activity against human colon cancer cell line HCT116, which is provided by protonated isoxazole **1′**.

This research was supported by The Ministry of Science and Higher Education of the Russian Federation (Agreement with the Zelinsky Institute of Organic Chemistry RAS no. 075-15-2020-803).

Online Supplementary Materials

Supplementary data associated with this article can be found in the online version at doi: 10.1016/j.mencom.2022.09.007.

References

1 P. Vitale and A. Scilimati, *Adv. Heterocycl. Chem.*, 2017, **122**, 1.
2 D. Giomi, F. M. Cordero and F. Machetti, in *Comprehensive Heterocyclic Chemistry III*, eds. A. R. Katritzky, C. A. Ramsden, E. F. V. Scriven and R. J. K. Taylor, Elsevier, Amsterdam, 2008, vol. 4, pp. 367–473.
3 A. V. Galenko, A. F. Khlebnikov, M. S. Novikov, V. V. Pakalnis and N. V. Rostovskii, *Russ. Chem. Rev.*, 2015, **84**, 335.
4 D. A. Vasilenko, K. N. Sedenkova, T. S. Kuznetsova and E. B. Averina, *Synthesis*, 2019, **51**, 1516.
5 A. Sysak and B. Obminska-Mrukowicz, *Eur. J. Med. Chem.*, 2017, **137**, 292.
6 M. A. Topchiy, G. K. Sterligov, A. A. Ageshina, S. A. Rzhevskiy, L. I. Minaeva, M. S. Nechaev and A. F. Asachenko, *Russ. Chem. Bull.*, 2022, **71**, 484.
7 M. Zimecki, U. Bąchor and M. Mączyński, *Molecules*, 2018, **23**, 2724.
8 J. Zhu, J. Mo, H.-Z. Lin, Y. Chen and H.-P. Sun, *Bioorg. Med. Chem.*, 2018, **26**, 3065.
9 D. A. Vasilenko, E. V. Dueva, L. I. Kozlovskaya, N. A. Zefirov, Y. K. Grishin, G. M. Butov, V. A. Palyulin, T. S. Kuznetsova, G. G. Karganova, O. N. Zefirova, D. I. Osolodkin and E. B. Averina, *Bioorg. Chem.*, 2019, **87**, 629.
10 D. A. Vasilenko, K. S. Sadovnikov, K. N. Sedenkova, D. S. Karlov, E. V. Radchenko, Y. K. Grishin, V. B. Rybakov, T. S. Kuznetsova, V. L. Zamoyski, V. V. Grigoriev, V. A. Palyulin and E. B. Averina, *Molecules*, 2021, **26**, 6411.
11 E. B. Averina, D. A. Vasilenko, Y. A. Gracheva, Y. K. Grishin, E. V. Radchenko, V. V. Burmistrov, G. M. Butov, M. E. Neganova, T. P. Serkova, O. M. Redkozubova, E. F. Shevtsova, E. R. Milaeva, T. S. Kuznetsova and N. S. Zefirov, *Bioorg. Med. Chem.*, 2016, **24**, 712.
12 A. P. Egorova and V. A. Makarov, *Russ. Chem. Bull.*, 2020, **69**, 635.
13 G. C. Arya, K. Kaur and V. Jaitak, *Eur. J. Med. Chem.*, 2021, **221**, 113511.
14 D. A. Vasilenko, E. B. Averina, N. A. Zefirov, B. Wobith, Yu. K. Grishin, V. B. Rybakov, O. N. Zefirova, T. S. Kuznetsova, S. A. Kuznetsov and N. S. Zefirov, *Mendeleev Commun.*, 2017, **27**, 228.
15 V. Spanò, R. Rocca, M. Barreca, D. Giallombardo, A. Montalbano, A. Carbone, M. V. Raimondi, E. Gaudio, R. Bortolozzi, R. Bai, P. Tassone, S. Alcaro, E. Hamel, G. Viola, F. Bertoni and P. Barraja, *J. Med. Chem.*, 2020, **63**, 12023.
16 D. V. Tsyganov, M. N. Semenova, L. D. Konyushkin, V. I. Ushkarov, M. M. Raihstat and V. V. Semenov, *Mendeleev Commun.*, 2019, **29**, 163.
17 N. B. Chernysheva, A. S. Maksimenko, F. A. Andreyanov, V. P. Kislyi, Y. A. Strelenko, V. N. Khrustalev, M. N. Semenova and V. V. Semenov, *Eur. J. Med. Chem.*, 2018, **146**, 511.
18 K. S. Sadovnikov, D. A. Vasilenko, Y. A. Gracheva, N. A. Zefirov, E. V. Radchenko, V. A. Palyulin, Y. K. Grishin, V. A. Vasilichin, A. A. Shtil, P. N. Shevtsov, E. F. Shevtsova, T. S. Kuznetsova, S. A. Kuznetsov, A. S. Bunev, O. N. Zefirova, E. R. Milaeva and E. B. Averina, *Arch. Pharm.*, 2022, **335**, 2100425.
19 V. V. Spiridonov, M. A. Orlova, I. A. Ivanov, I. G. Panova, A. P. Orlov, Yu. A. Antonova, T. P. Trofimova and A. A. Yaroslavov, *Colloids Surf., A*, 2020, **585**, 124104.
20 V. V. Spiridonov, M. I. Afanasov, L. A. Makarova, A. V. Sybachin and A. A. Yaroslavov, *Mendeleev Commun.*, 2021, **31**, 412.
21 S. D. Sokolov, G. B. Tikhomirova and K. F. Turchin, *Chem. Heterocycl. Compd.*, 1985, **21**, 507 (*Khim. Geterotsikl. Soedin.*, 1985, 609).
22 G. E. Kass and S. Orrenius, *Environ. Health Perspect.*, 1999, **107**, 25.
23 L. Bird, *Nat. Rev. Immunol.*, 2022, **22**, 144.

Received: 27th May 2022; Com. 22/6914